Journal of Medicinal Chemistry Article

J. Med. Chem. **2011,** *54,* 817–830 **817**
DOI: 10.1021/jm1012193

Discovery of Potent Competitive Antagonists and Positive Modulators of the P2X2 Receptor

Younis Baqi,[†,#] Ralf Hausmann,[‡,#] Christiane Rosefort,[‡] Jürgen Rettinger,[§] Günther Schmalzing,[‡] and Christa E. Müller*[,†]

[†]*PharmaCenter Bonn, Pharmaceutical Institute, Pharmaceutical Chemistry I, Pharmaceutical Sciences Bonn (PSB), University of Bonn, An der Immenburg 4, D-53121 Bonn, Germany,* [‡]*Department of Molecular Pharmacology, RWTH Aachen University, Wendlingweg 2, D-52074 Aachen, Germany, and* [§]*MultiChannelSystems MCS GmbH, Aspenhausstrasse 21, D-72770 Reutlingen, Germany.* [#] *These authors contributed equally.*

Received September 19, 2010

Evaluation and optimization of anthraquinone derivatives related to Reactive Blue 2 at P2X2 receptors yielded the first potent and selective P2X2 receptor antagonists. The compounds were tested for inhibition of ATP (10 μM) mediated currents in *Xenopus* oocytes expressing the rat P2X2 receptor. The most potent antagonists were sodium 1-amino-4-[3-(4,6-dichloro[1,3,5]triazine-2-ylamino)phenylamino]-9,10-dioxo-9,10-dihydroanthracene-2-sulfonate (**63**, PSB-10211, IC_{50} 86 nM) and disodium 1-amino-4-[3-(4,6-dichloro[1,3,5]triazine-2-ylamino)-4-sulfophenylamino]-9,10-dioxo-9,10-dihydroanthracene-2-sulfonate (**57**, PSB-1011, IC_{50} 79 nM). Compound **57** exhibited a competitive mechanism of action (pA_2 7.49). It was >100-fold selective versus P2X4, P2X7, and several investigated P2Y receptor subtypes ($P2Y_{2,4,6,12}$); selectivity versus P2X1 and P2X3 receptors was moderate (>5-fold). Compound **57** was >13-fold more potent at the homomeric P2X2 than at the heteromeric P2X2/3 receptor. Several anthraquinone derivatives were found to act as positive modulators of ATP effects at P2X2 receptors, for example, sodium 1-amino-4-(3-phenoxyphenylamino)-9,10-dioxo-9,10-dihydroanthracene-2-sulfonate (**51**, PSB-10129, EC_{50} 489 nM), which led to about a 3-fold increase in the ATP-elicited current.

Introduction

Purinergic receptors are a family of plasma membrane proteins, activated either by the nucleoside adenosine (P1 or adenosine receptors), or by nucleotide derivatives, such as ATP, ADP, UTP, and UDP (P2 or nucleotides receptors).[1] In addition, the nucleobase adenine has recently also been identified as a signaling molecule activating specific G protein-coupled receptors termed adenine or P0 receptors.[2]

The P2 purinergic receptors are further divided into two main subfamilies: ligand-gated ion channels or ionotropic receptors, termed P2X,[3a] and G protein-coupled or metabotropic receptors, designated P2Y.[3b] So far, seven subtypes in the P2X family (P2X1-7) and eight subtypes in the P2Y family ($P2Y_{1,2,4,6,11,12,13,14}$) have been identified.[3]

P2X receptors are membrane cation channels gated by extracellular ATP and are composed of homomeric or heteromeric assemblies of three subunits.[4] Recently, a crystal structure of the ATP-gated zebrafish P2X4 receptor channel was published in a 3 Å resolution in the closed state without ligand.[5] ATP has been proposed to bind to an intersubunit site ~45 Å from the ion channel domain, in a deep cleft, inducing conformational changes within and between subunits. These changes, in turn, may be propagated to the ion channel by conserved residues located at the transmembrane domain−extracellular domain interface.[5]

P2X2 receptors (P2X2Rs)[a] are widely distributed throughout the peripheral and central nervous system and on many non-neuronal cell types, where they play a role in sensory transmission and modulation of synaptic function. For instance, homomeric P2X2Rs facilitate excitatory transmission onto interneurons[6] and mediate sensory transmission from taste buds[7] and ventilatory responses.[8] P2X2R exhibit slow desensitization kinetics and are the only homomeric P2X subtype potentiated by acidic conditions; they are also potentiated by Zn^{2+} but inhibited by other divalent cations at high concentrations.[9] P2X2 subunits may form heterotrimeric channels with P2X3 or P2X6 subunits. P2X2R knockout mice have shown a reduced pain-related response in the second phase after intraplantar injection of formalin indicating potential effects of P2X2 antagonists on pain.[10] Inoue et al. showed that P2X2 antisense prevented mechanical allodynia induced by intraplantar injection of the P2X agonist α,β-methylene-ATP.[11] Furthermore, P2X2 knockout mice had reduced bladder distension reflexes, and antagonists acting at P2X2R might be useful for the treatment of urinary incontinence.[10]

In order to investigate the (patho)physiological role of homomeric P2X2Rs and to explore their potential as drug targets, potent and selective P2X2R antagonists are required.[12] While potent antagonists for P2X1, P2X3, and P2X7 receptor subtypes have recently been developed[12,13] no highly potent or selective P2X2R antagonists have been described to date.

*Address correspondence to Dr. Christa E. Müller, Pharmazeutisches Institut Pharmazeutische Chemie I An der Immenburg 4, D-53121 Bonn, Germany. Phone: +49-228-73-2301. Fax: +49-228-73-2567. E-mail: christa.mueller@uni-bonn.de.

[a] Abbreviations: AB-25, Acid Blue 25; *e*N, *ecto*-5′-nucleotidase; ESI, electrospray ionization; FCC, flash column chromatography; HPLC, high performance liquid chromatography; LC-MS, liquid chromatography−mass spectrometry; NMR, nuclear magnetic resonance; NPP(s), nucleotide pyrophosphatase(s); NTPDase(s), nucleoside triphosphate diphosphohydrolase(s); P2X2R(s), P2X2 receptor(s); rP2X receptor, rat P2X receptor; PSB, Pharmaceutical Sciences Bonn; RB-2, Reactive Blue 2; RB-4, Reactive Blue 4; RP-TLC, reversed phase thin layer chromatography; SAR(s), structure−activity relationship(s); TLC, thin layer chromatography; wt, wildtype.

Published on Web 01/05/2011

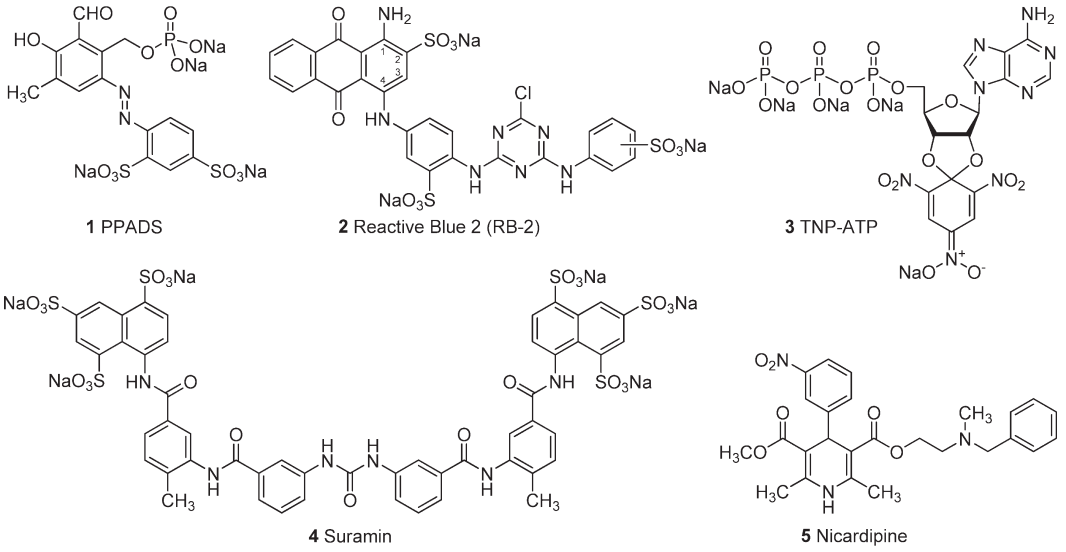

Figure 1. Structures of P2X2R antagonists.

PPADS (**1**), Reactive Blue 2 (RB-2, **2**), and TNP-ATP (**3**) (for structures see Figure 1) are approximately equipotent inhibitors of ATP-evoked currents through human or rat P2X2R (pIC_{50}'s range from 5.4 to 6.4), but much less potent than at the homomeric P2X1 or P2X3 channels.[14]

Suramin (**4**) has been reported to be of similar potency (pIC_{50} = 5.4−6.0) at P2X2R in some studies,[15] while others have reported suramin as having a 3−10-fold lower potency (pIC_{50} = 4.5−5.0) than these antagonists.[14a,b] In our assay, suramin inhibited oocyte-expressed rat P2X2R with a pIC_{50} value of 6.31 ± 0.01 (Supporting Information, Figure 1). The dihydropyridine derivative nicardipine (**5**), a calcium channel blocker, was shown to be an antagonist at recombinant rat P2X2R with an IC_{50} value of 25 μM and an about 10-fold lower inhibitory potency at P2X4 receptors.[16]

In addition to the moderate inhibitory potency of the anthraquinone dye RB-2 (**2**, Figure 1) at P2X2R (IC_{50}: 4 μM, see Table 3), it has been reported to act as an antagonist at other nucleotide receptor subtypes as well (P2X1, P2X4, $P2Y_1$, $P2Y_2$, $P2Y_4$, $P2Y_6$, $P2Y_{11}$, and $P2Y_{12}$ receptors).[16−31] Furthermore, **2** is a nonselective inhibitor of ectonucleotidases, including ecto-5′-nucleotidase (*e*N),[32] nucleoside triphosphate diphosphohydrolases (NTPDases),[33] and nucleotide pyrophosphatases (NPPs).[34]

It had previously been shown that the substitution pattern in the 4-position of the anthraquinone moiety plays an important role in the ability of the compounds to antagonize certain P2 receptor subtypes, such as P2X1 and $P2Y_1$-like,[35] $P2Y_2$,[29] and $P2Y_{12}$ receptors,[30,31] and to inhibit *e*N,[32] and NTPDase isoenzymes,[33] The modification of this substituent has, for example, led to the development of the most potent non-nucleotide-derived $P2Y_{12}$ antagonists known to date, which exhibit high selectivity versus other P2 receptors as well as *ecto*-nucleotidases.[30,31,36] Also this concept led to the development of potent and selective inhibitors of *e*N[32] endowed with high selectivity versus other *ecto*-nucleotidases as well as P2 receptors.[32] Thus, the anthraquinone scaffold appears to behave as a privileged structure in medicinal chemistry for nucleotide-binding protein targets.[32,37] Although **2** itself behaves as a so-called "frequent hitter" interacting with many different proteins, careful structural modification can successfully result in high selectivity for a single target. In the present study, we identified and developed the first potent and selective P2X2R antagonists starting from **2** as a lead structure.

Results and Discussion

Chemistry. Compounds were synthesized as depicted in Scheme 1. The preparation of compounds **7**, **10**−**14**, **17**−**24**, **27**, **29**−**31**, **33**−**49**, and **52**−**56** has previously been described.[29,32,33,38] The synthesis of products **8**, **9**, and **26** had been described in the literature[29,33] but has now been improved. Like the new compounds **15**, **16**, **25**, **28**, **32**, **50**, and **51**, they were obtained by a recently developed variant of the Ullmann coupling reaction.[28,39] The coupling of 4-bromo-substituted anthraquinone derivatives **6a** or **6b**[36] with the appropriate amine in phosphate buffer (pH 6−7) in the presence of Cu^0 under microwave irradiation at 80−120 °C for 5−20 min yielded the target compounds **7**−**56** (Scheme 1). Good to excellent isolated yields were obtained. The anilinoanthraquinone derivatives **39**, **40**, and **45**−**47**, which bear a primary amino group in the *m*- or *p*-position of the N^4-phenyl ring, were subsequently treated with cyanuric acid chloride (Scheme 1) to afford the desired products **57**, **58**, **60**, **61**, and **63**. Aniline derivatives **40** and **46** were further reacted with 2-bromopyrimidine yielding compounds **59** and **62** (Scheme 1).[30] Compound **58** was further treated with methanol at 60 °C for 30 min to yield **64** (Scheme 1).[30] Two of the dichlorotriazinyl derivatives (**57**, **61**) were hydrolyzed with water at 90 °C for 1 h to produce the corresponding diol derivatives **65** and **66** (Scheme 1).

The compounds were purified by flash column chromatography on reversed phase material. The purity of the compounds was determined by HPLC-MS/UV methods and a purity of at least 95% was confirmed. In Table 1 reaction times, isolated yields, and information on purity of the new compounds are collected.

Purification of Reactive Blue 4. Curiously, one of the most potent P2X2 antagonists of the present series of anthraquinone derivatives identified in this study, compound **57** (IC_{50} 0.079 μM, see below), is commercially available and known as Reactive Blue 4 (RB-4, CAS 13324-20-4). However, neither synthetic protocols nor spectral data for this compound have been available in the literature. Commercial RB-4 is not a pure compound and sold with a declared dye content of

Scheme 1. Syntheses of Target Compounds[a]

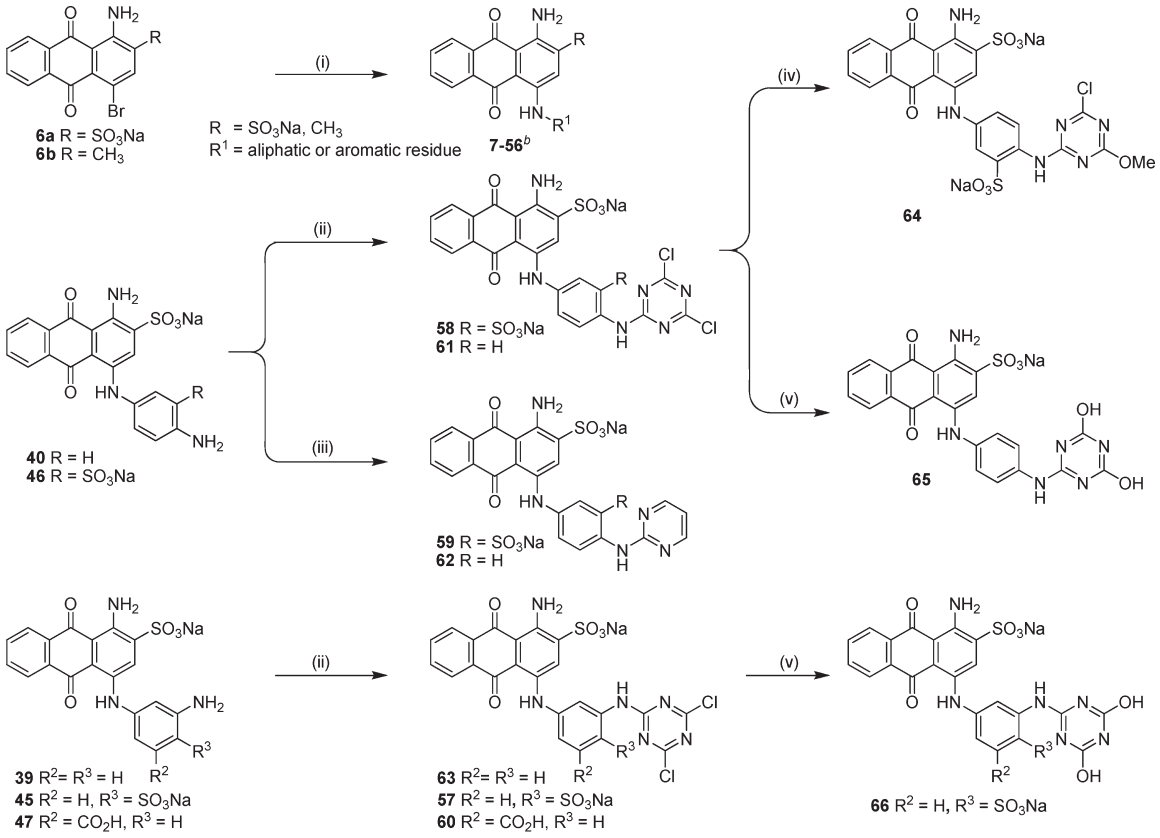

[a] Reagents and conditions: (i) amine, phosphate buffer, Cu^0, microwave, 80−120 °C, 5−20 min, yield 30−96%; (ii) cyanuric acid chloride, acetone: water (1:2), 0−5 °C, 1−6 h, yield 80−95%; (iii) 2-bromopyrimidine, acetone/water (1:2), 0−5 °C 1 h, then reflux, 1−3 days, yield 90−97%; (iv) MeOH, 60 °C, 30 min, yield 96%; (v) water, Na_2CO_3, 90 °C, 1 h, yield 95−97%. [b] For R and R^1 see Tables 1−3.

only 35% (Sigma-Aldrich), or ca. 40% (Alfa Aesar), respectively. Since **57** could be a very useful tool we developed − in addition to the total synthesis − a highly efficient and simple purification procedure of commercial RB-4 by reversed phase-18 flash column chromatography (RP-18 FCC, for details see Experimental Section). The chemical structure and purity were confirmed by LC-MS (96%), NMR, and RP-TLC and found to be identical to that of synthesized compound **57**. However, we discovered that the dye content of the commercial product had only been about 24%, since it was contaminated by its hydrolysis products, the dihydroxy-triazinyl derivative **66** (ca. 3%), and the corresponding monohydroxy-monochlorotriazinyl derivative (ca. 1%). Furthermore, it contained 72% of inorganic salts such as NaCl and sodium phosphate. Nevertheless, the purification is economically advantageous compared to the total synthesis of **57**, especially if larger amounts of the compound are required.

Biological Assays. The effect of the compounds on rat P2X2 and P2X4 receptor-mediated currents was analyzed by using two-electrode voltage-clamp electrophysiology in *Xenopus* oocytes transiently expressing the respective receptors as described before.[42] Further information about this functional assay is given in the Experimental Section. The rat rather than the human P2X receptors were used because rats or other rodents are frequently used in preclinical studies. The most active compound **57** was additionally investigated at rat P2X1, P2X3, P2X7, and heteromeric P2X2/3 receptors using the same methodology. In order to assess selectivity versus P2Y receptor subtypes as well, a series of compounds was investigated at recombinant $P2Y_2$, $P2Y_4$, $P2Y_6$ receptors in calcium mobilization assays using 1321N1 astrocytoma cells, and at $P2Y_{12}$ receptors in radioligand bindings studies at human platelet membrane preparations as previously described.[29−31,44,45]

Structure−Activity Relationships. RB-2 (**2**) is a negatively charged anthraquinone dye with three sulfonate groups and a molecular weight of 840.10 g/mol that binds to several P2 receptor subtypes and to various *ecto*-nucleotidases typically with micromolar affinity.[32,33] In the literature, it has been reported to antagonize P2X2R with an IC_{50}-value of 4 μM.[14a,d] We found that Acid Blue 25 (**7**), a much smaller molecule (416.38 g/mol) bearing only one sulfonate function was similarly potent (Table 2). In order to get more information on the structure−activity relationships (SAR) of this class of compounds as ligands of P2X2Rs and the related P2X4 subtype, the effects of a large series of alkyl-(aryl)amino-anthraquinone derivatives, structurally related to **2**, on P2X2 and P2X4 receptor-mediated currents were analyzed.[42]

AB-25 (**7**) is the simplest structure of the present series, in which ring D (phenyl ring on N^4 of the 4-aminoanthraquinone derivative) is not substituted, and the anthraquinone ring system bears a sulfonate group in the 2-position; when this group was replaced by a methyl group as in compounds **8** and **9** the inhibitory activity was also lost (Table 2). We therefore focused our attention on 2-sulfoanthraquinone derivatives. From initial screening of 49 different alkyl(aryl)amino-anthraquinone

Table 1. Reaction Times, Isolated Yields, Molecular Weights and Purity of Newly Synthesized Anthraquinone Derivatives

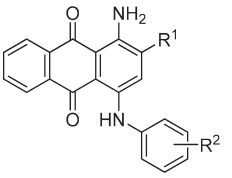

Structure A

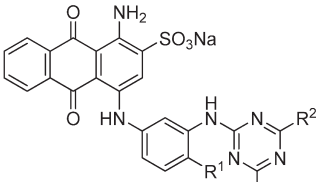

Structure B

compd	R^1	R^2	reaction time (min)	yield (%)[a]	MW (g/mol)	purity by LC-MS/UV(%)[b]
			Structure A			
8	CH_3	H	5	75	328.4	95.3
9	CH_3	CH_3	5	80	342.4	95.5
15	SO_3Na	3-trifluoromethyl	5	90	484.5	98.2
16	SO_3Na	3-ethyl	5	91	444.4	99.7
25	SO_3Na	3,5-dimethoxy	5	83	476.5	99.5
26	SO_3Na	2-ethoxy	5	80	460.5	98.5
28	SO_3Na	3-fluoro	5	96	434.4	99.9
32	SO_3Na	3,5-difluoro	5	75	452.4	99.2
50	SO_3Na	3-benzyl	10	65	506.5	99.2
51	SO_3Na	3-phenoxy	10	60	508.5	97.4
			Structure B			
57[c]	SO_3Na	Cl	15 + 30	55[d]	681.4	95.1
63[e]	H	Cl	5 + 15	57[d]	623.4	97.1
65	H	OH	5 + 120 + 60	61[d]	542.5	98.4
66[f]	SO_3Na	OH	15 + 30 + 60	53[d]	644.5	98.4

[a] Isolated yields. [b] A sample (10 μL) was injected into an HPLC column and elution was performed with a gradient of water/methanol (containing 2 mM NH_4CH_3COO) from 90:10 to 0:100 for 30 min at a flow rate of 250 μL/min, starting the gradient after 10 min. UV absorption was detected from 200 to 950 nm using a diode array detector. Purity of the compounds was determined at 254 nm. [c] Known as Reactive Blue 4 (RB-4) with a dye content of about 35−40%; neither synthesis nor spectral data have been published. [d] Total yield over two or three steps, respectively. [e] Compound was described in one publication as a coloring dye for poly(vinylalcohol); neither synthesis nor spectral data have been published.[40] [f] Compound described in the literature as a dye,[41] but no synthetic procedure nor spectral data have been provided.

derivatives at P2X2 and P2X4 receptors, it appeared that the SARs are restricted. All tested compounds were inactive (at 10 μM) at the P2X4 receptor. Most of the tested compounds exhibited moderate activity at the P2X2R in the range of 1−10 μM. A lipophilic substituent at the *o*- and/or *p*-position, such as fluoro (**29**), methyl (**12**, **14**), methoxy (**22**, **24**), ethoxy (**26**)), *di*-methyl (**17**, **18**) or *tri*-methyl (**48**), was tolerated. In addition, introducing a hydrophilic function (carboxy) in the *o*-, *m*-, or *p*-position (**35**−**37**), a sulfonate at the *p*-position (**34**) and an amino function at the *o*- or *m*-position (**38**, **39**) was also tolerated. Moreover, a combination of negatively charged residues (sulfonate, carboxy) with amino (**45**−**47**) or hydroxy (**54**) was tolerated as well. Introducing a large substituent in the *p*-position (**52**, **53**) did not improve the activity. Interestingly, the α-naphthyl- (**11**), *o*-sulpho- (**33**), and *p*-amino-substituted (**40**) derivatives were the only compounds which showed no activity at the P2X2R in the present series (Table 2). However, acetylation of the *p*-amino group in **40** yielding compound **41** resulted in a more than 15-fold increase in P2X2-inhibitory potency (IC_{50} 0.69 μM).

On the other hand, introducing a lipophilic substituent in the *m*-position, for example, methyl, methoxy, or chloro (**13**, **23**, **30**) increased the activity to the sub-micromolar range (IC_{50} < 1 μM), while trifluoromethyl, ethyl, bromo, and nitro in the *m*-position (**15**, **16**, **31**, **42**) and *di*-substition in the *m*-position with 3,5-*di*-methoxy or 3,5-*di*-fluoro residues (**25**, **32**) did not alter the activity.

A hydroxy substituent in the *p*-position (**21**) increased the activity (IC_{50} 0.588 μM) as well. A hydrogen-donating hydroxy (OH) group in the *p*-position appeared to be important for the activity, because blocking of this hydrogen donor with a methyl (*p*-methoxy, **24**) or phenyl (*p*-phenoxy, **27**) group decreased the activity. Introducing a carboxy group in the *m*-position in the presence of a *p*-hydroxy substitutent (**54**), decreased the activity as well (Table 2).

Interestingly, four compounds of the present study showed potentiation of the ATP induced P2X2 channel responses rather than inhibition of the channel. Three of these activators bear a lipophilic substituent in the *m*-position (**19**, **50**, and **51**), while one compound (**56**) has a *m*-sulfonate group on ring D and a phenylamino group in the *p*-position (**56**); see Table 2. Moderate effects were already seen at low concentrations of 100 nM of the test compound (106−132% increase, ATP effect set at 100%), while much higher effects could be observed at higher concentrations (see also Figure 6).

According to these SARs, a lipophilic substituent in the *m*-position of the N^4-phenyl ring may enhance inhibitory or modulatory activity, and a hydrophilic substituent (OH) in the *p*-position is favorable for good inhibitory activity as well. Therefore, several arylamino-anthraquinone derivatives having a lipophilic substituent in the *m*-position were synthesized and evaluated as antagonists at P2X2Rs (Table 3). For a systematic direct comparison, lipophilic *p*-substituted analogues were synthesized as well and evaluated at P2X2 and P2X4 receptors. Introducing a dichlorotriazinylamino moiety in the *m*-position in the presence of a sulfonate group in the *p*-position (**57**) led to the first potent and selective P2X2 antagonist (IC_{50} 79 nM) known so far.

A carboxy group in the *m*-position (in the presence of *m*-dichlorotriazinylamino substitution, **60**) also led to a potent and selective antagonist (IC_{50} 293 nM). A dichlorotriazinylamino substituent in the *p*-position in the presence of a sulfonate

Table 2. Pharmacological Evaluation of Selected Anthraquinone Derivatives at Rat P2X2 and P2X4 Receptors

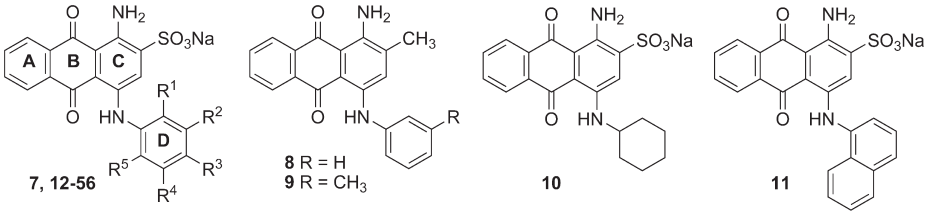

compd	R^1	R^2	R^3	R^4	R^5	IC_{50} rP2X2[a] (μM)	IC_{50} rP2X4[a] (μM)
7 (AB-25)	H	H	H	H	H	~1−10	> 10
8			see structure above			> 10	> 10
9			see structure above			> 10	> 10
10			see structure above			~1−10	> 10
11			see structure above			> 10	> 10
12	CH_3	H	H	H	H	~1−10	> 10
13	H	CH_3	H	H	H	~0.8	> 10
14	H	H	CH_3	H	H	~1−10	> 10
15	H	CF_3	H	H	H	> 1	n.d.[d]
16	H	CH_2CH_3	H	H	H	> 1	n.d.[d]
17	CH_3	CH_3	H	H	H	~1−10	> 10
18	CH_3	H	CH_3	H	H	~1−10	> 10
19	H	CH_3	H	CH_3	H	potentiating effect 106% at 100 nM[c]	n.d.[d]
20	OH	H	H	H	H	~1−10	> 10
21	H	H	OH	H	H	**0.588** (0.511−0.677)[b]	> 10
22 (PSB-716)[49]	OCH_3	H	H	H	H	~2	> 10
23	H	OCH_3	H	H	H	**0.623** (0.540−0.719)[b]	> 10
24	H	H	OCH_3	H	H	**1.73** (1.38−2.17)[b]	> 10
25	H	OCH_3	H	OCH_3	H	> 1	n.d.[d]
26	OC_2H_5	H	H	H	H	~1−10	> 10
27	H	H	OC_6H_5	H	H	~1−10	> 10
28	H	F	H	H	H	> 1	n.d.[d]
29	H	H	F	H	H	~1−10	> 10
30	H	Cl	H	H	H	~0.1−0.3	n.d.[d]
31	H	Br	H	H	H	~1−10	> 10
32	H	F	H	F	H	> 1	n.d.[d]
33	SO_3Na	H	H	H	H	> 10	> 10
34	H	H	SO_3Na	H	H	~1−10	> 10
35	CO_2H	H	H	H	H	~1−10	> 10
36	H	CO_2H	H	H	H	~1−10	> 10
37	H	H	CO_2H	H	H	~1−10	> 10
38	NH_2	H	H	H	H	~1−10	> 10
39	H	NH_2	H	H	H	~1−10	> 10
40	H	H	NH_2	H	H	> 10	> 10
41	H	H	$NHC(O)CH_3$	H	H	0.69	> 10
42	H	NO_2	H	H	H	> 1	n.d.[d]
43	CO_2H	H	Cl	H	H	~1−10	> 10
44	CO_2H	H	H	Cl	H	~1−10	> 10
45	H	NH_2	SO_3Na	H	H	~1−10	> 10
46	H	SO_3Na	NH_2	H	H	~1−10	> 10
47	H	CO_2H	H	NH_2	H	~1−10	> 10
48	CH_3	H	CH_3	H	CH_3	~1−10	> 10
49	CH_3	NH_2	CH_3	H	CH_3	~1−10	> 10
50	H	$CH_2C_6H_5$	H	H	H	potentiating effect 120% at 100 nM[c]	n.d.[d]
51	H	OC_6H_5	H	H	H	potentiating effect 132% at 100 nM[c]	n.d.[d]
52	H	H	CH_2CO_2H	H	H	~1−10	> 10
53	H	H	$CH_2P(=O)(OEt)_2$	H	H	~1−10	> 10
54	H	CO_2H	OH	H	H	~1−10	> 10
55	CH_3	NH_2	H	H	H	~1−10	> 10
56	H	SO_3Na	NHC_6H_5	H	H	potentiating effect 110% at 100 nM[c]	n.d.[d]

[a] Potencies of anthraquinone derivatives at rat P2X receptors recombinantly expressed in *Xenopus laevis* oocytes ($n \geq 5$). [b] 95% confidence interval (CI). [c] Percent potentiation of the ATP-induced current at indicated concentration of compound. [d] n.d. = not determined.

Table 3. Potency of Compounds Bearing Two Aromatic Rings (D and E) Connected to the Antraquinone Core Structure at Rat P2X2 and P2X4 Receptors

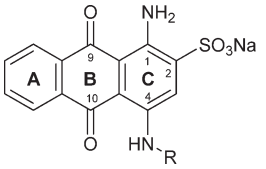

Compd.	R	IC_{50} rP2X2[a] (μM)	IC_{50} rP2X4[a] (μM)	Compd.	R	IC_{50} rP2X2[a] (μM)	IC_{50} rP2X4[a] (μM)
57 (PSB-1011)		**0.079** (0.068–0.090)	> 10	**64**	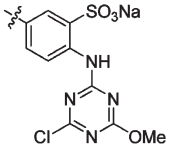	**0.582** (0.451–0.751)[b]	> 10
58	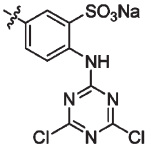	**1.16** (1.12–1.21)	> 10	**65**	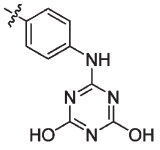	**0.197** (0.176–0.221)[b]	> 10
59	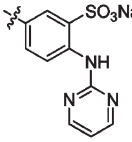	~ 1–10	> 10				
60	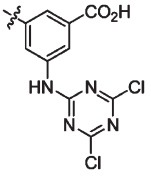	**0.293** (0.261–0.329)[b]	> 10	**66**	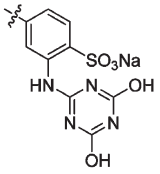	~ 0.3–1.0	n.d.[c]
				67 (Cibacron Blue 3GA)	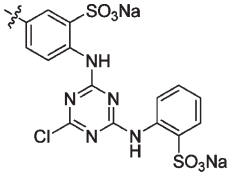	> 1	40
61	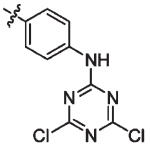	**0.117** (0.106–0.130)	> 10				
62	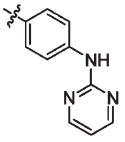	> 1	> 10	**2** Reactive Blue 2 (RB-2)	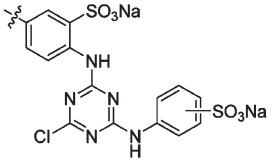	**4**[26-29]	n.d.[c]
63 (PSB-10211)	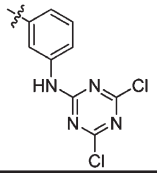	**0.086** (0.076–0.098)	n.d.[c]				

[a] Potencies of aryl(alkyl)anthraquinone derivatives at rat P2X receptors recombinantly expressed in *Xenopus laevis* oocytes ($n \geq 3$). [b] 95% confidence interval (CI). [c] n.d. = not determined.

group in the *m*-position yielded **58**, which exhibited an IC_{50} value of 1.16 μM. Formal removing of the sulfonate group in the *m*-position of **58** providing **61** improved the activity by 10-fold (IC_{50} 117 nM), indicating that a sulfonate group on ring D was not required and even detrimental. Replacing a chlorine atom in **58** by a methoxy group (**64**) slightly improved the potency (0.582 μM). Hydrolysis of both chlorine atoms of compounds **61** and **57** to the corresponding dihydroxy-triazinyl derivatives **65** and **66** decreased the activity by ca. 2-fold (compare **61**/**65**), and > 4-fold (compare **57**/**66**).

Introducing a pyrimidine ring instead of a dichlorotriazinyl residue in the presence or absence of a sulfonate group in the *m*-position (**59**, **62**) decreased the activity. A direct analogue of **57** without a sulfonate group on ring D was synthesized (compound **63**) and evaluated at $P2X_2R$. As expected it showed a very good inhibitory activity (IC_{50} 0.086 μM, see

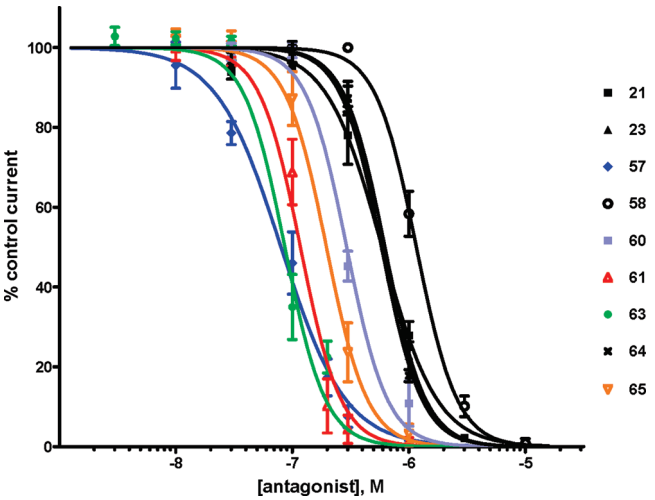

Figure 2. Concentration−response curves of selected P2X2R antagonists as assessed from stationary current (steady state) measurements. Concentration−inhibition curves were generated from agonist-induced current measurements in the presence of incrementally larger concentrations of the indicated antagonists. The extent of inhibition was judged from the ratio of the maximal and minimal stationary current in the absence and presence of antagonist, respectively. The continuous lines represent nonlinear curve fits by the Hill equation to the pooled data points from $n = 5-7$ experiments.

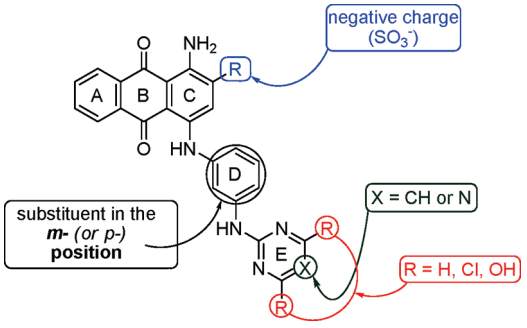

Figure 3. Structure−activity relationships of anthraquinone derivatives at rat P2X2Rs.

Table 3 and Figure 2) and was actually − besides compound **57** − the most potent inhibitor of the present series indicating that a sulfonate group on ring D was not required for high inhibitory potency.

To date, there are no known selective or highly potent P2X2R antagonists. So far, only PPADS (**1**), RB-2 (**2**), TNP-ATP (**3**), and suramin (**4**) were reported as moderately potent antagonists ($pIC_{50} = 5.4-4.4$, $IC_{50} = 4-40\ \mu M$) at P2X2Rs. These compounds are well-known to block almost all P2X receptor subtypes, and some are even blocking P2Y receptor subtypes as well. We now identified the first potent and selective rat P2X2R antagonist with nanomolar potency, compound **57** (IC_{50} P2X2 = 79 nM). It is highly selective versus the $P2Y_{12}$ receptor (> 200-fold) and the P2X4 receptor subtype (> 125-fold). Also, we have discovered that the direct analogue of **57**, compound **63**, shows a very similar potency at the P2X2R with an IC_{50} value of 86 nM. Figure 3 summarizes the SARs of the compounds as P2X2R antagonists. A substituent in the *m*-position of phenyl ring D is well accepted. Especially lipophilic substituents in the *m*-position increased the affinity. An aromatic ring (E) in the *meta*-position was accommodated well in the binding pockets of

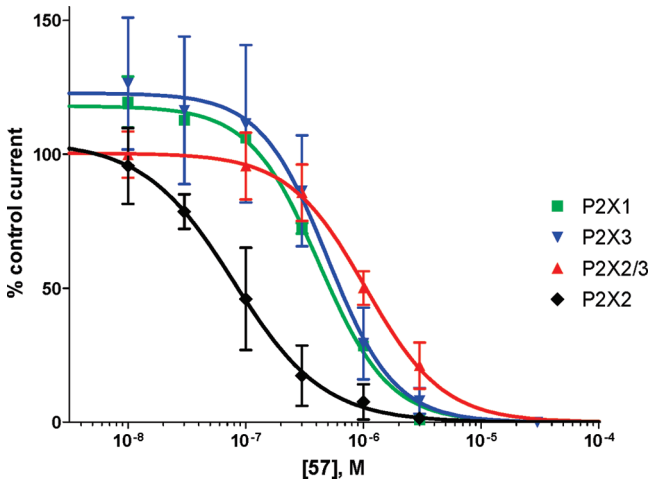

Figure 4. Potencies of compound **57** at different rP2X receptor isoforms as assessed from stationary current (steady state) measurements. Concentration−inhibition curves were generated from agonist-induced current measurements in the presence of incrementally larger concentrations of **57**. The extent of inhibition was judged from the ratio of the maximal and minimal stationary current in the absence and in the presence of **57**, respectively. Green square, rP2X2-X1 (rP2X1); black diamond, rP2X2; red triangle, rP2X2/3; blue triangle, rP2X2-X3 (rP2X3); The continuous lines represent nonlinear curve fits by the Hill equation to the pooled data points from $n = 5-7$ experiments. For convenience, all IC_{50} values of **57** are summarized in Table 4.

Table 4. Potencies of **57** at Recombinant P2X Receptor Subtypes

	IC_{50}, nM[a] (95% confidence interval)	selectivity vs P2X2
rP2X2-X1 (*P2X1*)	**422** (340−525)	5.3
wt-rP2X2	**79.2** (47−133)	
rP2X2-X3 (*P2X3*)	**494** (339−721)	6.2
wt-rP2X2/3	**1042** (810−1339)	13.2
wt-rP2X4	> 10,000	≫120
wt-rP2X7	> 10,000	≫120

[a] IC_{50} values were calculated from data of 5−7 independent experiments. For experimental details see Figure 4 and Experimental Section.

the P2X2Rs, while compounds substituted in the *p*-position were found to be less potent in most cases. Previously, we have shown that the binding site of the $P2Y_{12}$ receptor required a negative charge (SO_3^- or CO_2^-) in the *meta*-position besides an aromatic substituent in the *para*-position of ring D[30,31,36] indicating that SARs for $P2Y_{12}$ and P2X2Rs are very different. Recently, we have developed novel *ecto*-5′-nucleotidase inhibitors based on an anthraquinone scaffold.[32] The characteristics of the SARs for this enzyme target showed the requirement of a big lipophilic substituent (naphthyl or anthracenyl) attached directly to N^4 of the anthraquinone moiety, indicating the existence of a big lipophilic pocket in the active site of the enzyme.[32] Thus, all three targets are showing very different characteristic properties regarding the binding site for anthraquinone derivatives. This enables us to develop selective antagonists and inhibitors.

Selectivity. To determine the P2X receptor subtype selectivity of the most potent P2X2R-blocking compound **57** in this series, concentration inhibition curves were generated at the homomeric rP2X1, rP2X2, rP2X3, rP2X4, and rP2X7 receptors, as well as the heteromeric rP2X2/3 receptor subtype (Figure 4). P2X5 receptors were not studied because the P2X5 subunit occurs in humans predominantly as an

Table 5. Selectivity of the Most Potent P2X2R Ligands vs Other P2 Receptor Subtypes

	IC_{50} (μM)				$K_i \pm$ SEM (μM) vs [^{3}H]PSB-0413
compd	$P2X_2$[a]	$P2Y_2$[b,29,32]	$P2Y_4$[b,32]	$P2Y_6$[a,32]	$P2Y_{12}$[b,30,31]
2	4.0[26−29]	1.85 ± 0.39	9.79 ± 3.91	4.34 ± 0.89	0.68 ± 0.26
7	∼1−10	11.0 ± 1.0	25.8 ± 14.3	84.6 ± 9.0[d]	9.83 ± 2.43
13	∼0.8	> 10	> 10	3.92 ± 1.28	∼10
21	0.588 ± 0.083	4.63 ± 0.53	2.22 ± 1.12[d]	5.30 ± 1.00	∼10
23	0.623 ± 0.090	∼10	∼10	≫10	∼10
30	∼0.1−0.3	24.5 ± 10.4	21.8 ± 2.3	≫10	6.76 ± 2.07
50	potentiating effect 120% at 100 nM[e]	≫10	> 10	≫10	n.d.[c]
51	potentiating effect 132% at 100 nM[e]	∼10	n.d.[c]	4.56 ± 0.18	n.d.[c]
57	0.079 ± 0.011	∼10	> 10	≫10	17.1 ± 7.8
60	0.293 ± 0.034	3.27 ± 0.76	1.45 ± 0.38	2.55 ± 1.33	3.76 ± 1.03
61	0.117 ± 0.012	12.1 ± 1.4	∼10	∼10	1.90 ± 0.24
63	0.086 ± 0.011	24.3 ± 3.5	∼10	> 10	n.d.[c]
64	0.582 ± 0.156	24.2 ± 3.5	> 10	≫10	0.66 ± 0.12
65	0.197 ± 0.023	∼30	∼10	n.d.[c]	n.d.[c]

[a] Rat receptor. [b] Human receptors. [c] n.d. = not determined. [d] $n = 2$. [e] Percent potentiation of the ATP-induced current at indicated concentration of compound.

assembly deficient natural deletion mutant.[46] P2X6 receptors were omitted because P2X6 does not form functional homomeric channels under most circumstances.[9] To assess inhibition of P2X1 and P2X3 receptors also under steady-state conditions, non-desensitizing rP2X2-X1 and rP2X2-X3 receptor chimeras were used, in which the N-terminal tail including the first transmembrane domain is replaced by the complementary portion of the rP2X2 subunit. Since the ligand-binding ectodomain originates entirely from the rP2X1 or the rP2X3 subunit, these chimeras can be reliably used as non-desensitizing substitutes of wt-rP2X1 and rP2X3 receptors.[13e] ATP served as an agonist for all receptors, with the exception of non-desensitizing heteromeric rP2X2/3 receptors that were selectively activated by α,β-methylene-ATP (α,β-meATP, 1 μM) to avoid activation of coexpressed homomeric rP2X2Rs that respond to ATP, but are virtually resistant to activation by α,β-meATP (for details, see Experimental Section).[9] Concentration−inhibition curves and IC_{50} values were derived from nonlinear least-squares fits of the Hill equation to the pooled data points and yielded the following rank order of potencies (Figure 4) for compound **57**: wt-rP2X2 > non-desensitizing mutant of rP2X1 ≥ non-desensitizing mutant of rP2X3 > wt-rP2X2/3 > > wt-rP2X4, wt-rP2X7. Compound **57** was virtually ineffective in blocking rP2X4 or rP2X7 receptor mediated currents (< 10% inhibition at 10 μM of inhibitor, data not shown). As depicted in Figure 4, low concentrations (10−100 nM) of compound **57** slightly potentiated P2X1 and P2X3 receptor mediated currents. However, in the absence of ATP compound **57** elicited no P2X1 or P2X3 receptor responses.

Thus, compound **57** was highly selective for P2X2R versus P2X4 and P2X7 receptor subtypes (> 120-fold), while it was moderately selective versus P2X1 and P2X3 receptors (5−6-fold). Interestingly, **57** was 13-fold selective for the homomeric P2X2 receptor compared with the heteromeric P2X2/3 receptor and may therefore be used to distinguish between effects mediated by the homomeric and those induced by the heteromeric P2X2-subunits containing subtypes. The significantly (> 10-fold) different potency of **57** at heteromeric P2X2/3 receptors compared to P2X2 receptors is not totally unexpected as the known subunit composition of two P2X3 and one P2X2 subunit combined with the intersubunit ligand

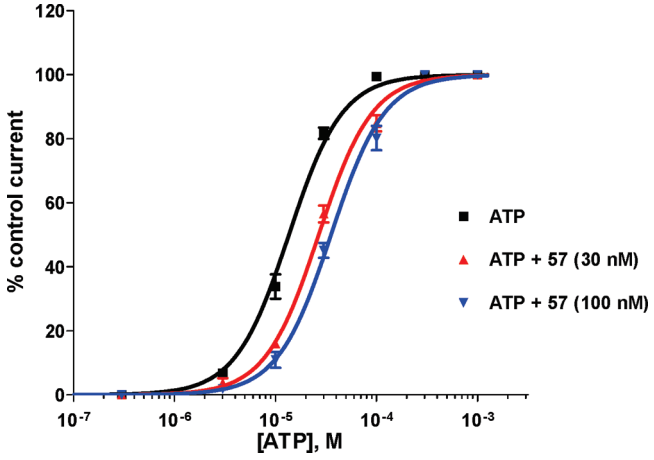

Figure 5. Assessment of the mechanism of inhibition of rP2X2Rs induced by **57**. ATP concentration−response curves were established by stimulating oocytes expressing rP2X2Rs with incrementally larger concentrations of ATP in the absence (black square, $EC_{50} = 13.8 \pm 0.9\,\mu M$, $n_H = 1.8 \pm 0.1$, $n = 5$) and in the presence of 30 nM **57** (red triangle, $EC_{50} = 26.9 \pm 2.1\,\mu M$, $n_H = 1.5 \pm 0.1$, $n = 5$) and 100 nM **57** (blue triangle, $EC_{50} = 35.7 \pm 3.4\,\mu M$, $n_H = 1.5 \pm 0.1$, $n = 5$). Currents were normalized to those elicited by a saturating concentration of 1 mM ATP. A simultaneous (global) fit yielded a pA_2 value of 7.49. In noninjected control oocytes, ATP elicits no current both in the absence and presence of up to 3 μM compound **57** (data not shown).

binding site implies that no pure "P2X2 binding site" is present in these heteromeric channels.

In addition selected, potent compounds were further investigated at some P2Y receptor subtypes (Table 5) as previously described.[29−32]

The initial lead compound **2** (RB-2) exhibited similar inhibitory potency at the P2X2 receptor as at the investigated P2Y receptor subtypes in the low micromolar range. The much smaller anthraquinone derivative **7** (sodium 1-amino-4-phenylamino-9,10-dioxo-9,10-dihydroanthracene-2-sulfonate, AB-25) was similarly potent at P2X2R, but somewhat weaker (3−20-fold) at the P2Y receptors, thus showing increased P2X2 selectivity. The same was true for several simple, small anthraquinone derivatives, including **13**, **21**, **23**, and **30**. Selectivity appeared to be even more pronounced for most

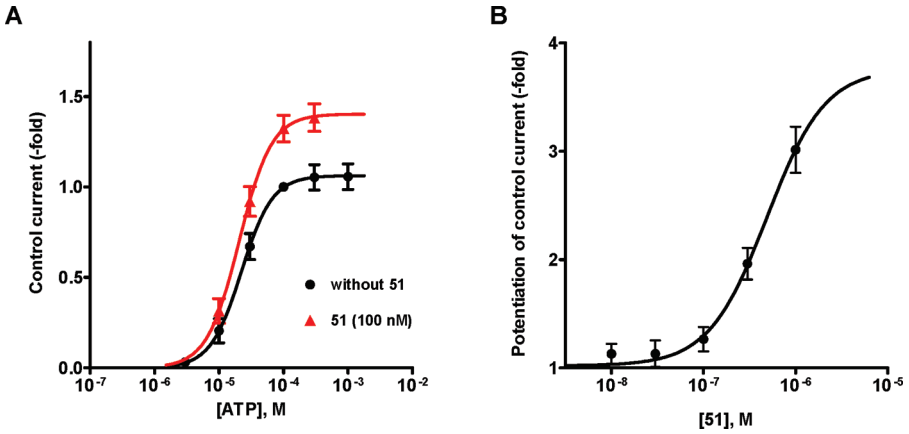

Figure 6. Potentiating effect of **51** on ATP-elicited rP2X2R mediated currents. (A) ATP concentration−response analysis in the absence and presence of 100 nM **51**. ATP concentration−response curves were established by stimulating oocytes expressing the rP2X2R with incrementally larger concentrations of ATP in the absence of **51** (black circle, $EC_{50} = 22.2 \pm 2.4\,\mu M$, $n_H = 1.8 \pm 0.1$, $n = 6$) or in the presence of 100 nM **51** (red triangle, $EC_{50} = 20.6 \pm 2.7\,\mu M$, $n_H = 1.7 \pm 0.2$, $n = 6$). Currents were normalized to those elicited by a saturating concentration of 1 mM ATP in the absence of **51**. The continuous lines represent nonlinear curve fits by the Hill equation to the pooled data points from $n = 6$ experiments. (B) Concentration−response analysis of **51** in the presence of 10 μM ATP. Currents were elicited by repetitive application of 10 μM ATP in the presence of incrementally larger concentrations of compound **51**. Currents were normalized to those elicited by 10 μM ATP in the absence of **51**. The continuous line represents a nonlinear curve fit by the Hill equation to the pooled data points from $n = 5$ experiments. An EC_{50} value of 489 ± 90 nM ($n_H = 1.4 \pm 0.4$, $n = 5$) was determined.

of the larger, more potent anthraquinone derivatives bearing an additional ring E (e.g., **57**, **60**, **61**, **63**, **65**). The most potent compound of the present series, **57**, was more than 120-fold selective versus the investigated $P2Y_2$, $P2Y_4$, $P2Y_6$, and $P2Y_{12}$ receptor subtypes.

Mechanism of Action. To delineate whether compound **57** acts as a competitive rP2X2R antagonist, ATP concentration−response curves were established in the absence and in the presence of **57**. In these experimental series ATP activated rP2X2R mediated inward currents with an EC_{50} value of 13.8 ± 1.5 μM. In noninjected control oocytes ATP elicits no current both in the absence and presence of up to 3 μM compound **57** (data not shown). Increasing concentrations of compound **57** progressively shifted ATP concentration−response curves parallel to the right without changing the maximal response (Figure 5). These data are in agreement with a competitive mechanism of action of compound **57** at the rP2X2R. However, we cannot completely exclude an allosteric modulation of the ATP affinity by **57** because the rightward shift decreases at the higher concentration of **57**. A global fit of the concentration response data yielded a pA_2 value of 7.49 as an estimate of the antagonistic potency independent of any particular mechanism.

Compounds with Positive Modulatory Action at rP2X2Rs. As shown in Table 2 coapplication of a low concentration of 100 nM of compounds **19**, **50**, **51**, and **56** showed increased ATP elicited current amplitudes (106−132% of control current (application of ATP alone, 100%)). To further characterize this effect, we determined concentration−response curves for the most active modulator **51**. Compound **51** (up to 1 μM) showed no agonistic effect of its own if applied without ATP (data not shown). As shown in Figure 6A, the ATP potency in this experimental series in the presence of 100 nM **51** ($EC_{50} = 20.6 \pm 2.7\,\mu M$, $n_H = 1.7 \pm 0.2$, $n = 6$) was not significantly altered as compared to the ATP potency in the absence of **51** ($EC_{50} = 22.2 \pm 2.4\,\mu M$, $n_H = 1.8 \pm 0.1$, $n = 6$). However, 100 nM of **51** led to a significant increase in the maximum current amplitudes. Repetitive activation of rP2X2Rs by 10 μM ATP in the presence of incrementally larger concentrations of compound **51** yielded an EC_{50} value of 489 ± 90 nM for potentiation of ATP-elicited currents (Figure 6B). The increase in efficacy without effect on the potency of ATP may be compatible with an allosteric modulatory effect. On the other hand, the 3-fold increase by 1 μM of compound **51** in the current amplitude elicited by 10 μM ATP is difficult to reconcile with a purely allosteric mechanism. Therefore, further experiments are needed to fully resolve the specific mechanism of action of these positive modulatory compounds.

Conclusions

In conclusion, a series of anthraquinone derivatives was investigated at P2X2 receptors. Analysis of structure−activity relationships and compound optimization yielded the first potent P2X2 receptor antagonists. Among the 59 investigated compounds, 11 are new compounds not previously described in the literature, while several others, including **57**, **63**, and **66**, can be found in databases as dyes; however, neither synthetic procedures nor spectral data have been published, and they have probably not been obtained in high purity required for pharmacological testing. Most of the synthesized compounds (52 compounds) were potent P2X2R antagonist, 33 showing IC_{50} values in the low micromolar range (ca. 1−10 μM), and 11 even in the moderate to low nanomolar range (0.079−0.83 μM). This study led to the discovery of compound **57**, which is the most potent P2X2R antagonist known to date showing a competitive mechanism of action ($IC_{50} = 79$ nM, $pA_2 = 7.49$). In fact, **57** is the first highly potent antagonist for this channel showing high (> 100-fold) selective versus the closely related P2X4 and P2X7 receptor ion channels and versus several investigated P2Y receptor subtypes ($P2Y_{2,4,6,12}$). Moderate selectivity of **57** versus P2X1 and P2X3 receptors (> 5-fold) was also observed. The P2X2 antagonist **57** was considerably (> 13-fold) more potent at the homomeric as compared to the heteromeric P2X2/3 receptor. Furthermore, several anthraquinone derivatives were discovered to act as positive modulators of ATP effects at P2X2 receptors, the most potent being **51**, which led to an about 3-fold increase in the maximal ATP-elicited current with an EC_{50} value of 489 nM.

The new P2X2 receptor modulators will be useful as pharmacological tools for studying P2X2R and the potential of P2X2R antagonists and enhancers as novel drugs.

Experimental Section

Chemistry. Material and Methods. All materials were used as purchased (Acros, Alfa Aesar or Sigma-Aldrich, Germany). Thin-layer chromatography was performed using TLC aluminum sheets silica gel 60 F_{254}, or TLC aluminum sheets RP silica gel 18 F_{254} (Merck, Darmstadt, Germany). Colored compounds were visible at daylight; other compounds were visualized under UV light (254 nm). Flash chromatography was performed on a Büchi system using silica gel RP-18 (Merck, Darmstadt, Germany). ^{1}H- and ^{13}C NMR data were collected on a Bruker Avance 500 MHz NMR spectrometer at 500 MHz (^{1}H), or 126 MHz (^{13}C), respectively. DMSO-d_6 was used as a solvent. Chemical shifts are reported in parts per million (ppm) relative to the deuterated solvent; that is, DMSO, δ ^{1}H: 2.49 ppm; ^{13}C: 39.7 ppm, coupling constants J are given in Hertz and spin multiplicities are given as s (singlet), d (doublet), t (triplet), q (quartet), m (multiplet), br (broad).

The purities of isolated products were determined by ESI− mass spectra obtained on an LCMS instrument (Applied Biosystems API 2000 LCMS/MS, HPLC Agilent 1100) using the following procedure: the compounds were dissolved at a concentration of 0.5 mg/mL in H_2O: MeOH = 1:1, containing 2 mM NH_4CH_3COO. Then, 10 μL of the sample was injected into an HPLC column (Phenomenex Luna 3 μ C18, 50 × 2.00 mm). Elution was performed with a gradient of water/methanol (containing 2 mM NH_4CH_3COO) from 90:10 to 0:100 for 30 min at a flow rate of 250 μL/min, starting the gradient after 10 min. UV absorption was detected from 200 to 950 nm using a diode array detector. Purity of all compounds was determined at 254 nm. A second HPLC method was used to confirm purity as previously described.[35] For microwave reactions a CEM Focused Microwave Synthesis type Discover apparatus was used. A freeze-dryer (CHRIST ALPHA 1−4 LSC) was used for lyophilization. The purity of the compounds proved to be ≥95%. The syntheses of compounds **7**, **10**−**14**, **17**−**24**, **27**, **29**−**31**, **33**−**49**, and **52**−**58**, **60**, **61**, and **63** has previously been described.[29,32,33,38] All other compounds were newly prepared in analogy to described methods.[30,38,39]

Purification of Reactive Blue 4 (RB-4). RB-4 was obtained from Alfa Aesar (A12911) and subsequently purified. Initially an RP-TLC was obtained using 40% aqueous acetone as eluent; the R_f value of the main blue spot was 0.5. In a second step, 250 mg of RB-4 was dissolved in ca. 10 mL of water and injected onto a Sepacore Glass Column C-690 (ID 26 × 460 mm) three-quarter filled with reversed phase-18 silica gel (40−63 μm, Merck) and purified by flash column chromatography. Initially, water was used as an eluent and the polarity was gradually decreased by increasing the concentration of acetone form 0% to 5, 10, 20, and finally to 40%. The collected main blue-colored fractions corresponding to the blue band that appeared last on the column were pooled and evaporated under vacuum at 25 °C to remove the acetone. The remaining water was subsequently removed by lyophilization yielding 60 mg (yield: 24%) of pure **57** as a blue powder.

General Procedures for the Preparation of 4-Substituted Anthraquinones (7−56). General Procedure A. To a 5 mL microwave reaction vial equipped with a magnetic stirring bar were added bromo-substituted compounds (bromaminic acid sodium salt **6a**, or the methyl, **6b**) (0.20 mmol) and the appropriate aniline and/or amine derivative (0.40 mmol, 2 equiv), followed by a buffer solution of Na_2HPO_4 (pH 9.6) (4.5 mL) and NaH_2PO_4 (pH 4.2) (0.5 mL). A catalytic amount (ca. 0.002−0.003 g) of finely powdered elemental copper was added. The mixture was capped and irradiated in the microwave oven (80−100 W) for 5−20 min at 80−120 °C. Then the reaction mixture was cooled to rt, and the product was purified using the following procedure. The contents of the vial were filtered to remove the elemental copper. Then ca. 200 mL of water was added to the filtrate and the aqueous solution was extracted with dichloromethane (200 mL). The extraction procedure was repeated until the dichloromethane layer became colorless (2−3 times). Then the aqueous layer was reduced by rotary evaporation to a volume of 10−20 mL, which was subsequently submitted to flash column chromatography using RP-18 silica gel and water as an eluent. The polarity of the eluent was then gradually decreased by the addition of methanol or acetone in the following steps: 5, 10, 20, 40, 60, and 80%. Fractions containing blue product were collected. For some compounds, the last step of purification (RP-18 flash chromatography) had to be repeated two to three times to obtain pure product (≥95% purity as determined by LC-MS). The pooled product-containing fractions were evaporated under a vacuum to remove the methanol or acetone, and the remaining water was subsequently removed by lyophilization to yield (up to 96%) as blue powders (Scheme 1 and Table 2).

General Procedure B. Coupling reaction of cyanuric acid chloride with the amino function in phenyl ring D: synthesis of ABCDE ring anthraquinone derivatives **57**, **58**, **60**, **61**, and **63** was achieved analogous to the previously described procedure.[30] An ice-cooled solution of cyanuric acid chloride (1.0 mmol) in water (25 mL) and acetone (25 mL) was added to a stirred solution of amine-containing compound (**39**, **40**, and **45**−**47**) (0.5 mmol) in water (25 mL) at 0−5 °C. The resulting mixture was stirred for 1 h at 0−5 °C, then allowed to warm up to rt and kept stirring at rt for 1−2 h. The formation of product was monitored by RP-TLC using a mobile phase of acetone/water (2:3). After completion of the reaction, the solvents were evaporated and the residue was purified by flash column chromatography on RP-18 silica gel using acetone/water as an eluent to obtain the desired products (**57**, **58**, **60**, **61**, and **63**) (Scheme 1).

General Procedure C. The coupling reaction of 2-bromopyrimidine with the amino function in phenyl ring D: synthesis of ABCDE ring anthraquinone derivatives **59** and **62** was achieved as previously described.[30] In brief: an ice-cooled solution of 2-bromopyrimidine (1.0 mmol) in water (25 mL) and acetone (25 mL) was added to a stirred solution of the respective compound (**39** or **46**) (0.5 mmol) in water (25 mL) at 0−5 °C. Then the temperature was gradually increased to refluxing at 120 °C for 1−3 days. After completion of the reaction, the solvents were evaporated and the residue was purified by flash column chromatography on RP-18 silica to obtain the desired products **59**, and **62**, in excellent (90−97%) isolated yield (Scheme 1).

General Procedure D. Hydrolysis of the dichlorotriazine moiety to the corresponding dihydroxytriazine group. A 0.05 mmol of dichlorotriazine containing compounds (**57** or **61**) was dissolved in water (15 mL) then heated to 90 °C, followed by the addition of 10 mg of Na_2CO_3 (2 equiv) and stirring at that temperature for 1 h. After completion of the reaction, RP-TLC control, the mixture was subjected to flash column chromatography using RP-18 silica to obtain the desired products **65** or **66**, in excellent (95−97%) isolated yield (Scheme 1).

Synthesis and Spectral Data of the Key Compounds. Sodium 1-Amino-4-(3-benzylphenylamino)-9,10-dioxo-9,10-dihydroanthracene-2-sulfonate (50). Reaction conditions: According to the general procedures A: 5 min, 120 °C, 100 W; pressure up to 10 bar. Analytical data: mp > 300 °C, blue powder. ^{1}H NMR: δ 3.96 (s, 2H, CH_2), 7.04 (d, 1H, 4′-H), 7.10 (d, 1H, 6′-H), 7.15 (br, 1H, 2′-H), 7.18 (m, 1H, 4″-H), 7.29 (m, 4H, 2″-H, 3″-H, 5″-H, 6″-H), 7.84 (m, 2H, 6-H, 7-H), 8.05 (s, 1H, 3-H), 8.26 (m, 2H, 5-H, 8-H), 10.10 (br, 2H, 1-NH_2), 12.03 (s, 1H, 4-NH). ^{13}C NMR: δ 41.1 (CH_2), 109.3 (C-9a), 111.5 (C-4a), 120.6, 122.9, 123.5, 125.0, 126.08, 126.13, 126.2, 128.7, 129.0, 129.8, 132.9 (C-2′, C-6′, C-3, C-5, C-8, C-4′, C-5′, C1″, C-2″, C-3″, C-4″, C-5″,

C-6″), 133.3, 133.7, 134.3, 139.4 (C-8a, C-10a, C-6, C-7), 140.9 (C-1′), 143.0 (C-4), 143.2 (C-2), 144.5 (C-1), 181.9 (C-9), 182.6 (C-10). LC-MS (*m*/*z*): 502 [M-Na + NH_4^+]$^+$, 485 [M − Na]$^+$, 483 [M − Na]$^-$. Purity by HPLC-UV (254 nm)-ESI-MS: 99.2%.

Sodium 1-Amino-4-(3-phenoxyphenylamino)-9,10-dioxo-9,10-dihydroanthracene-2-sulfonate (51). Reaction conditions: According to the general procedures A: 5 min, 120 °C, 100 W; pressure up to 10 bar. Analytical data: mp >300 °C, blue powder. ^{1}H NMR: δ 6.79 (dd, 1H, 4′-H), 6.88 (dd, 1H, 2′-H), 7.03 (dd, 1H, 6′-H), 7.12 (m, 3H, 2″-H, 4″-H, 6″-H), 7.42 (m, 3H,5′-H, 3″-H, 5″-H), 7.84 (m, 2H, 6-H, 7-H), 8.06 (s, 1H, 3-H), 8.25 (m, 2H, 5-H, 8-H), 10.01 (br, 2H, 1-NH_2), 11.86 (s, 1H, 4-NH). ^{13}C NMR: δ 109.4 (C-9a), 112.2 (C-4a), 112.5, 114.1, 117.5, 119.2, 123.1, 123.9, 126.1, 126.2, 130.3, 131.1 (C-3, C-5, C-8, C-2′, C-6′, C-4′, C-5′, C-2″, C-3″, C-4″, C-5″, C-6″), 133.0, 133.4, 133.6, 134.3 (C-8a, C-10a, C-6, C-7), 140.1 (C-1′), 141.2 (C-4), 142.8 (C-2), 144.6 (C-1), 156.1, 158.0 (C-3′, C1″), 182.1 (C-9), 182.9 (C-10). LC-MS (*m*/*z*): 504 [M − Na + NH_4^+]$^+$, 487 [M − Na]$^+$, 485 [M − Na]$^-$. Purity by HPLC-UV (254 nm)-ESI-MS: 97.4%.

Disodium 1-Amino-4-[3-(4,6-dichloro[1,3,5]triazine-2-ylamino)-4-sulfophenylamino]-9,10-dioxo-9,10-dihydroanthracene-2-sulfonate (57). According to the general procedure B: An ice-cooled solution of cyanuric acid chloride (184.4 mg, 1.0 mmol) in water (25 mL) and acetone (25 mL) was added to a stirred solution of disodium 1-amino-4-(3-amino-4-sulfophenylamino)-9,10-dioxo-9,10-dihydroanthracene 2-sulfonate (**45**) (256 mg, 0.5 mmol) in water (25 mL) at 0−5 °C. The resulting mixture was stirred for 1 h at 0−5 °C, then allowed to warm up to rt and kept stirring at rt for 2 h. The formation of product was monitored by RP-TLC using a mobile phase of acetone/water (2:3). After completion of the reaction the solvents were evaporated and the residue was purified by flash column chromatography on RP-18 silica gel using acetone:water as an eluent yielded 289 mg (yield 85%) of a blue powder, mp >300 °C. ^{1}H NMR: δ 7.04 (dd, 1H, 6′-H), 7.70 (d, 1H, 5′-H), 7.84 (m, 3H, 6-H, 7-H, 2′-H), 8.04 (s, 1H, 3-H), 8.27 (m, 2H, 5-H, 8-H), 10.82 (br, 2H, 1-NH_2), 11.98 (br, 1H, 4-NH). ^{13}C NMR: δ 109.4 (C-9a), 112.2 (C-4a), 117.5 (C-2′), 118.3 (C-3′), 123.0 (C-6′), 126.17 (C-8), 126.21 (C-5), 128.1 (C-5′), 133.0 (C-4′), 133.4 (C-6), 133.6 (C-7), 134.2 (C-10a), 134.3 (C-8a), 134.5 (C-1′), 140.0 (C-3′), 140.1 (C-4), 142.8 (C-2), 144.6 (C1), 153.0 (C-1″), 154.4 (C-3″, C-5″), 182.1 (C-9), 183.0 (C-10). LC-MS (*m*/*z*): 654 [M − 2Na + NH_4^+]$^+$, 637 [M − 2Na]$^+$, 635 [M − 2Na]$^-$. Purity by HPLC-UV (254 nm)-ESI-MS: 96.0%.

Sodium 1-Amino-4-[3-(4,6-dichloro[1,3,5]triazine-2-ylamino)-phenylamino]-9,10-dioxo-9,10-dihydroanthracene-2-sulfonate (63). According to the general procedure B: An ice-cooled solution of cyanuric acid chloride (184.4 mg, 1.0 mmol) in water (25 mL) and acetone (25 mL) was added to a stirred solution of sodium 1-amino-4-(3-aminophenylamino)-9,10-dioxo-9,10-dihydroanthracene 2-sulfonate (**39**) (216 mg, 0.5 mmol) in water (25 mL) at 0−5 °C. The resulting mixture was stirred for 15 min at 0−5 °C. The formation of product was monitored by RP-TLC using a mobile phase of acetone:water (2:3). After completion of the reaction the solvents were evaporated and the residue was purified by flash column chromatography on RP-18 silica gel using acetone:water as an eluent yielded 275 mg (yield 95%) of a blue powder, mp >300 °C. ^{1}H NMR: δ 7.07 (m, 1H, H-5′), 7.40 (m, 2H, H-4′, H-6′), 7.47 (m, 1H, H-2′), 7.84 (m, 2H, H-6, H-7), 8.01 (s, 1H, H-3), 8.27 (m, 2H, H-5, H-8), 10.82 (br, 1H, NH-3), 12.01 (br, 1H, NH-4). ^{13}C NMR: δ 109.4 (C-9a), 111.8 (C-4a), 115.8 (C-2′), 117.4 (C-5′), 118.8 (C-3), 122.9 (C-6′), 126.2 (C-5, C-8), 130.1 (C-4′), 133.0 (C-6), 133.4 (C-7), 133.7 (C-10a), 134.3 (C-8a), 138.7 (C-1′), 140.0 (C-3′), 140.6 (C-4), 142.9 (C-2), 144.5 (C1), 152.8 (C-1″), 154.1 (C-3″, C-5″), 182.0 (C-9), 182.8 (C-10). LC-MS (*m*/*z*): 575 [M − Na + NH_4^+]$^+$, 555 [M − Na]$^-$, 557 [M − Na]$^+$. Purity by HPLC-UV (254 nm)-ESI-MS: 97.1%.

Sodium 1-Amino-4-[4-(4,6-dihydroxy[1,3,5]triazine-2-ylamino)-phenylamino]-9,10-dioxo-9,10-dihydroanthracene-2-sulfonate (65). According to the general procedure D: 29 mg 0.05 mmol of Sodium 1-amino-4-[4-(4,6-dichloro-[1,3,5]triazine-2-ylamino)phenylamino]-9,10-dioxo-9,10-dihydroanthracene-2-sulfonate (**61**) was dissolved in water (15 mL) then heated to 90 °C, followed by the addition of Na_2CO_3 (10 mg, 2 equiv.) and let to stirr at 90 °C for 1 h. After completion of the reaction, RP-TLC control using a mobile phase of acetone:water (2:3), the mixture was subjected to flash column chromatography on RP-18 silica gel using acetone:water as an eluent yielded 26 mg (yield 95%) of a blue powder, mp >300 °C. ^{1}H NMR: δ 7.09 (d, 2H, 2′-H, 6′-H), 7.83 (m, 2H, 6-H, 7-H), 7.85 (d, 2H, 3′-H, 5′-H), 7.94 (s, 1H, 3-H), 8.27 (m, 2H, 5-H, 8-H), 8.6 (br, 1H, OH), 8.8 (br, 1H, OH), 10.17 (br, 2H, 1-NH_2), 12.16 (s, 1H, 4-NH). ^{13}C NMR: δ 109.0 (C-9a), 110.2 (C-4a), 120.0 (C-2′, C-6′), 122.8 (C-5), 124.1 (C-3′, C-5′), 126.0, 126.1, 131.2, 132.7, 133.0 (C-3, C-6, C-7, C-8, C-4′), 133.9 (C-10a), 134.3 (C-8a), 139.4, 142.6, 143.2, 144.3 (C-1, C-2, C-4, C-1′), 160.9 (C-1″), 167.0 (C-3″, C-5″), 181.7 (C-9, C-10). LC-MS (*m*/*z*): 538 [M − Na + NH_4^+]$^+$, 520 [M − Na]$^+$, 518 [M − Na]$^-$. Purity by HPLC-UV (254 nm)-ESI-MS: 95.5%.

Disodium 1-Amino-4-[3-(4,6-dihydroxy-[1,3,5]triazine-2-ylamino)-4-sulfophenylamino]-9,10-dioxo-9,10-dihydroanthracene-2-sulfonate (66). According to the general procedure D: 34 mg 0.05 mmol of Disodium 1-amino-4-[3-(4,6-dichloro-[1,3,5]triazine-2-ylamino)-4-sulfophenylamino]-9,10-dioxo-9,10-dihydroanthracene-2-sulfonate (**57**) was dissolved in water (15 mL) then heated to 90 °C, followed by the addition of Na_2CO_3 (10 mg, 2 equiv.) and let to stirr at 90 °C for 1 h. After completion of the reaction, RP-TLC control using a mobile phase of acetone: water (2:3), the mixture was subjected to flash column chromatography on RP-18 silica gel using acetone:water as an eluent yielded 31 mg (yield 97%) of a blue powder, mp >300 °C. ^{1}H NMR: δ 7.02 (dd, 1H, 6′-H), 7.70 (d, 1H, 5′-H), 7.85 (m, 3H, 6-H, 7-H, 2′-H), 8.03 (s, 1H, 3-H), 8.27 (m, 2H, 5-H, 8-H), 10.75 (br, 1H, 3′-NH), 11.99 (br, 1H, 4-NH). ^{13}C NMR: δ 109.4 (C-9a), 112.1 (C-4a), 117.2 (C-2′), 118.2 (C-5′), 122.9 (C-3), 126.16 (C-6′), 126.22 (C-5, C-8), 128.0 (C-4′), 132.9 (C-6), 133.4 (C-7), 133.7 (C-10a), 134.0 (C-8a), 134.3 (C-1′), 134.8 (C-3′), 140.0 (C-4), 142.8 (C-2), 144.6 (C1), 153.4 (C-1″), 154.6 (C-3″, C-5″), 182.1 (C-9), 183.0 (C-10). LC-MS (*m*/*z*): 601 [M − 2Na]$^+$, 599 [M − 2Na]$^-$, 299 [M − 2Na]$^{2-}$. Purity by HPLC-UV (254 nm)-ESI-MS: 98.4%.

Biological Assays

Expression of P2X Receptors in *Xenopus laevis* Oocytes. Oocyte expression plasmids encoding wild type and hexahistidyl-tagged rat P2X subunits (rP2X2, rP2X3, rP2X4, rP2X7) were available from previous studies.[13e] Chimeric constructs rP2X2$^{1-47}$X1$^{48-399}$ and rP2X2$^{1-47}$X3$^{42-397}$ encoding amino acids Met^1-Val^{47} of the rP2X2 subunit joined in frame with ^{48}Val-^{399}Ser of the 399-amino acids rP2X1 subunit or ^{42}Val-^{397}His of the 397-amino acids rP2 × 3 subunit, respectively, have also been described previously.[13e] For expression of P2X receptors capped cRNAs were synthesized and injected into collagenase-defolliculated *Xenopus laevis* oocytes using a Nanoliter 2000 injector (WPI) as described previously.[13e] For expression of the heteromeric rP2X2/3 receptor, a 1:2 (w/w) ratio of rP2X2 and rP2X3 cRNA was injected. Oocytes were cultured at 19 °C in sterile oocyte Ringer's solution (ORi: 90 mM NaCl, 1 mM KCl, 1 mM $CaCl_2$, 1 mM $MgCl_2$, and 10 mM Hepes, pH 7.4) supplemented with 50 μg/mL of gentamycin.

Two-Electrode Voltage-Clamp Electrophysiology. Two to three days after cRNA injection, current responses were evoked by ATP (rP2X1, rP2X2, rP2X3, rP2X4, and rP2X7) or α,β-meATP (rP2X2/3) as indicated. Recordings were performed at ambient temperature (21−24 °C) by a conventional two-electrode voltage-clamp (TEVC) with a Turbo TEC-05 amplifier (npi Electronics) or by the Roboocyte automated electrophysiology system[47] (MultiChannelSystems MCS GmbH, Reutlingen, Germany) at a holding potential of −60 mV as

described previously.[13e] Oocytes were continuously perfused by gravity flow (5−10 mL/min) in a small flow-through chamber (volume about 10 μL) or in a round-bottom well of a 96-well plate, respectively, with a nominally calcium-free ORi solution (designated Mg-ORi), in which $CaCl_2$ was replaced by equimolar $MgCl_2$ to avoid a contribution of endogenous Ca^{2+}-dependent Cl^- channels to the ATP response. Dilutions of agonists and antagonists in Mg-ORi were prepared daily and applied by bath perfusion. Switching between bath solutions was controlled by a set of magnetic valves, enabling computer-controlled applications of compounds (CellWork Lite 5.1 software, NPI Electronics; Roboocyte system, MultiChannelSystems). As wt-rP2X1 and wt-rP2X3 receptors, once activated, desensitize rapidly in the continued presence of agonist, the current transient is too short to allow reaching a binding equilibrium between the coapplied compounds. To assess inhibition of P2X1 and P2X3 receptors also reliable under steady-state conditions, non-desensitizing rP2X2-X1 and rP2X2-X3 receptor chimeras were used, in which the N-terminal tail including the first transmembrane domain is replaced by the complementary portion of the rP2X2 subunit.[13e] Since the ligand-binding ectodomain originates entirely from the rP2X1 or the rP2X3 subunit, these chimeras can be reliably used as non-desensitizing substitutes of wt-rP2X1 and rP2X3 receptors. For concentration−inhibition analysis of nondesensitizing P2X2-X1, P2X2, P2X2/3, P2X2-X3, and P2X7 receptors or partial desensitizing P2X4 receptors, oocytes expressing the specified P2X receptor were superfused with agonist-containing (P2X2-X1 and P2X2-X3, 10 nM ATP; P2X2 and P2X4, 10 μM ATP; P2X7, 100 μM ATP) bath solution until a steady-state current was obtained. Then, the superfusion solution was switched to one containing both antagonist and the same concentration of agonist as before. The superfusion was maintained until a steady-state level of inhibition was reached, followed by switching to bath solution containing the agonist alone for washout of test compounds. Figure 7 shows representative original current traces of oocytes expressing homomeric rP2X2 receptors to illustrate this steady state protocol exemplarily. The percentage of the control response was calculated as the steady-state currents in the absence and presence of antagonist. For analysis of heteromeric P2X2/3 receptors the same steady-state protocol was used but with 1 μM α,β-meATP as agonist. Coexpression of rP2X2 and rP2X3 subunits results in a mixed population of heterogeneous receptors; these include both the homomeric rP2X2 and rP2X3 receptors as well as the heteromeric rP2X2/3 receptor. To exclude a contribution of the homomeric rP2X2 receptor to the current response, 1 μM α,β-meATP was used as an agonist, which activates the heteromeric rP2X2/3 receptor with > 100-fold higher potency than the homomeric rP2X2 receptor. Control experiments with oocytes injected solely with cRNA for the rP2X2 subunit confirmed that > 30 μM α,β-meATP was needed to evoke significant inward currents in these cells (data not shown). Any contribution of the homomeric rP2X3 receptor to the α,β-meATP-induced inward current was suppressed by repetitive α,β-meATP applications that hold the P2X3 receptor in the fully desensitized state.

Data Analysis. Data were plotted and fitted using Prism4 (GraphPAD Software Inc., San Diego, CA) and Origin 6.0. Agonist concentration−response curves were produced by measuring the maximal current induced by increasing concentrations of agonist, which were then normalized to the maximal current value obtained with a saturating ATP concentration. Concentration−response curves and half-maximal effective agonist concentrations (EC_{50}) were obtained from curves by iteratively fitting the Hill equation (eq 1) to the normalized data points pooled from several (n) oocytes

$$I/I_{max} = 1/(1 + ([EC_{50}/A])^{nH}) \quad (1)$$

where I is the current evoked by agonist concentration A, I_{max} the maximal current response, and n_H the Hill coefficient.

Concentration−inhibition curves and IC_{50} values were derived from nonlinear least-squares fits of eq 2 to the pooled data points

$$I_{Ant}/I_{max} = 1/(1 + ([Ant]/IC_{50})^{nH}) \quad (2)$$

where I_{max} is the current response in absence of antagonist (Ant), I_{Ant} is the current response at the respective antagonist concentration, and IC_{50} the antagonist concentration causing 50% inhibition of the current elicited by a given agonist concentration.

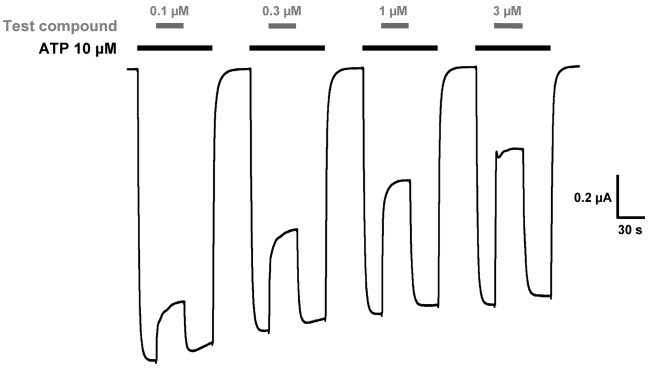

Figure 7. Steady state protocol for the assessment of the inhibitory potency of test compounds from stationary current measurements. A representative original current trace of an oocyte expressing rP2X2 receptors is shown. After a stationary current was elicited by application of 10 μM ATP (black bars), an incrementally larger concentration of the test compound (0.1−3 μM, gray bars) was coapplied with 10 μM ATP. The current declined until a new steady state was reached, indicating that inhibition by the test compound was fully developed. Then 10 μM ATP alone was applied for washout of the test compound until a new steady state was reached. The extent of inhibition was judged for each concentration of the test compound from the ratio of the maximal and minimal stationary current in the absence and presence of the test compound, respectively.

Experimental Procedures for Testing of Compounds at $P2Y_2$, $P2Y_4$, and $P2Y_6$ Receptors. Astrocytoma cell lines stably transfected with either the human $P2Y_2$, the human $P2Y_4$, or the rat $P2Y_6$ receptor were used.[29,43,44] Test compounds were investigated by measuring their inhibition of $P2Y_2$, $P2Y_4$, or $P2Y_6$ receptor-mediated intracellular calcium mobilization as previously described.[29,44,45]

Acknowledgment. Y.B. was supported by a DAAD (Deutscher Akademischer Austauschdienst) scholarship. C.E.M. and Y.B. are grateful for support by the Deutsche Forschungsgemeinschaft (DFG, GRK804). Meike Welz, Natalie Poryo, Karen Schmeling, and Dr. Anja B. Scheiff are acknowledged for testing selected compounds at P2Y receptors.

Supporting Information Available: Concentration−response curve for suramin at P2X2R, synthesis and spectral data of new

compounds as well as ^{1}H NMR and ^{13}C NMR spectra of newly synthesized anthraquinone derivatives. This material is available free of charge via the Internet at http://pubs.acs.org.

References

(1) (a) Burnstock, G. Physiology and pathophysiology of purinergic neurotransmission. *Physiol. Rev.* **2007**, *87*, 659–797. (b) Brunschweiger, A.; Müller, C. E. P2 receptors activated by uracil nucleotides−an update. *Curr. Med. Chem.* **2006**, *13*, 289–312.

(2) Borrmann, T.; Abdelrahman, A.; Volpini, R.; Lambertucci, C.; Alksnis, E.; Gorzalka, S.; Knospe, M.; Schiedel, A. C.; Cristalli, G.; Müller, C. E. Structure-activity relationships of adenine and deazaadenine derivatives as ligands for adenine receptors, a new purinergic receptor family. *J. Med. Chem.* **2009**, *52*, 5974–5989.

(3) (a) Khakh, B. S.; Burnstock, G.; Kennedy, C.; King, B. F.; North, R. A.; Séguéla, P.; Voigt, M.; Humphrey, P. P. International Union of Pharmacology. XXIV. Current status of the nomenclature and properties of P2X receptors and their subunits. *Pharmacol. Rev.* **2001**, *53*, 107–118. (b) Abbracchio, M. P.; Burnstock, G.; Boeynaems, J. M.; Barnard, E. M.; Boyer, J. L.; Kennedy, C.; Knight, G. E.; Fumagalli, M.; Gachet, C.; Jacobson, K. A.; Weisman, G. A. International Union of Pharmacology LVIII: update on the P2Y G protein-coupled nucleotide receptors: from molecular mechanisms and pathophysiology to therapy. *Pharmacol. Rev.* **2006**, *58*, 281–341.

(4) (a) Nicke, A.; Bäumert, H. G.; Rettinger, J.; Eichele, A.; Lambrecht, G.; Mutschler, E.; Schmalzing, G. P2X$_1$ and P2X$_3$ receptors form stable trimers: a novel structural motif of ligand-gated ion channels. *EMBO J.* **1998**, *17*, 3016–3028. (b) Benjamin Marquez-Klaka, B.; Rettinger, J.; Nicke, A. Inter-subunit disulfide cross-linking in homomeric and heteromeric P2X receptors. *Eur. Biophys. J.* **2009**, *38*, 329–338.

(5) Kawate, T.; Michel, J. C.; Birdsong, W. B.; Gouaux, E. Crystal structure of the ATP-gated P2X$_4$ ion channel in the closed state. *Nature* **2009**, 592–598.

(6) Khakh, B. S.; Gittermann, D.; Cockayne, D. A.; Jones, A. ATP modulation of excitatory synapses onto interneurons. *J. Neurosci.* **2003**, *23*, 7426–7437.

(7) Finger, T. E.; Danilova, V.; Barrows, J.; Bartel, D. L.; Vigers, A. J.; Stone, L.; Hellekant, G.; Kinnamon, S. C. ATP signaling is crucial for communication from taste buds to gustatory nerves. *Science* **2005**, *310*, 1495–1499.

(8) Rong, W.; Gourine, A. V.; Cockayne, D. A.; Xiang, Z.; Ford, A. P.; Spyer, K. M.; Burnstock, G. Pivotal role of nucleotide P2X2 receptor subunit of the ATP-gated ion channel mediating ventilatory responses to hypoxia. *J. Neurosci.* **2003**, *23*, 11315–11321.

(9) Gever, J. R.; Cockayne, D. A.; Dillon, M. P.; Burnstock, J.; Ford, A. P. D. W. Pharmacology of P2X channels. *Pflugers Arch. − Eur. J. Physiol.* **2006**, *452*, 513–537.

(10) Cockayne, D. A.; Dunn, P. M.; Zhong, Y.; Rong, W.; Hamilton, S. G.; Knight, G. E.; Ruan, H.-Z.; Ma, B.; Yip, P.; Nunn, P.; McMahon, S. P.; Burnstock, G.; Ford, A. P. D. W. P2X$_2$ knockout mice and P2X$_2$/P2X$_3$ double knockout mice reveal a role for the P2X2 receptor subunit in mediating multiple sensory effects of ATP. *J. Physiol.* **2005**, *567*, 621–639.

(11) Inoue, K.; Tsuda, M.; Koizumi, S. ATP induced three types of pain behaviors, including allodynia. *Drug Dev. Res.* **2003**, *59*, 56–63.

(12) (a) Jarvis, M. F.; Khakh, B. S. ATP-gated P2X cation-channels. *Neuropharmacology* **2009**, *56*, 208–215. (b) Burnstock, G. Purinergic signalling and disorders of the central nervous system. *Nat. Rev. Drug Discovery* **2008**, *7*, 575–590.

(13) (a) Volpini, R.; Mishra, R. C.; Kachare, D. D.; Ben, D. D.; Lambertucci, C.; Antonini, I.; Vittori, S.; Marucci, G.; Sokolova, E.; Nistri, A.; Cristalli, G. Adenine-Based Acyclic Nucleotides as Novel P2X$_3$ Receptor Ligands. *J. Med. Chem.* **2009**, *52*, 4596–4603. (b) Braun, K.; Rettinger, J.; Ganso, M.; Kassack, M.; Hildebrandt, C.; Ullmann, H.; Nickel, P.; Schmalzing, G.; Lambrecht, G. NF449: a subnanomolar potency antagonist at recombinant rat P2X$_1$ receptors. *Naunyn-Schmiedeberg's Arch. Pharmacol.* **2001**, *364*, 285–290. (c) Jarvis, M. F.; Burgard, E. C.; McGaraughty, S.; Honore, P.; Lynch, K.; Brennan, T. J .; Subieta, A.; van Biesen, T.; Cartmell, J.; Bianchi, B.; Niforatos, W.; Kage, K.; Yu, H.; Mikusa, J.; Wismer, C. T.; Zhu, C. Z.; Chu, K.; Lee, C.-H.; Stewart, A. O.; Polakowski, J.; Cox, B. F.; Kowaluk, E.; Williams, M.; Sullivan, J.; Faltynek, C. A-317491, a novel potent and selective non-nucleotide antagonist of P2X$_3$ and P2X$_{2/3}$ receptors, reduces chronic inflammatory and neuropathic pain in the rat. *Proc. Natl. Acad. Sci. U. S. A.* **2002**, *99*, 17179–17184. (d) Honore, P.; Mikusa, J.; Bianchi, B.; McDonald, H.; Cartmell, J.; Faltynek, C.; Jarvis, M. F. TNP-ATP, a potent P2X$_3$ receptor antagonist, blocks acetic acid-induced abdominal constriction in mice: comparison with reference analgesics. *Pain* **2002**, *96*, 99–105. (e) Hausmann, R.; Rettinger, J.; Gerevich, Z.; Meis, S.; Kassack, M. U.; Illes, P.; Lambrecht, G.; Schmalzing, G. The suramin analog 4,4′,4″,4‴-(carbonylbis(imino-5,1,3-benzenetriylbis (carbonylimino)))tetra-kis-benzenesulfonic acid (NF110) potently blocks P2X$_3$ receptors: subtype selectivity is determined by location of sulfonic acid groups. *Mol. Pharmacol.* **2006**, *69*, 2058–2067. (f) Stokes, L.; Jiang, L.-H.; Alcaraz, L.; Bent, J.; Bowers, K.; Fagura, M.; Furber, M.; Mortimore, M.; Lawson, M.; Theaker, J.; Laurent, C.; Braddock, M.; Surprenant, M. Characterization of a selective and potent antagonist of human P2X$_7$ receptors, AZ11645373. *Br. J. Pharmacol.* **2006**, *149*, 880–887. (g) King, B. F. Novel P2X$_7$ receptor antagonists ease the pain. *Br. J. Pharmacol.* **2007**, *151*, 565–567. (h) Baxter, A.; Bent, J.; Bowers, K.; Braddock, M.; Brough, S.; Fagura, M.; Lawson, M.; McInally, T.; Mortimore, M.; Robertson, M.; Weaver, R.; Webborn, P. Hit-to-Lead studies: The discovery of potent adamantane amide P2X$_7$ receptor antagonists. *Bioorg. Med. Chem. Lett.* **2003**, *13*, 4047–4050.

(14) (a) Bianchi, B. R.; Lynch, K. J.; Touma, E.; Niforatos, W.; Burgard, E. C.; Alexander, K. M.; Park, H. S.; Yu, H.; Metzger, R.; Kowaluk, E.; Jarvis, M. F.; van Biesen, T. Pharmacological characterization of recombinant human and rat P2X receptor subtypes. *Eur. J. Pharmacol.* **1999**, *376*, 127–138. (b) King, B. F.; Wildman, S. S.; Ziganshina, L. E.; Pintor, J.; Burnstock, G. Effects of extracellular pH on agonism and antagonism at a recombinant P2X$_2$ receptor. *Br. J. Pharmacol.* **1997**, *121*, 1445–1453. (c) Lynch, K. J.; Touma, E.; Niforatos, W.; Kage, K. L.; Burgard, E. C.; van Biesen, T.; Kowaluk, E. A.; Jarvis, M. F. Molecular and functional characterization of human P2X(2) receptors. *Mol. Pharmacol.* **1999**, *56*, 1171–1181. (d) Virginio, C.; Robertson, G.; Surprenant, A.; North, R. A. Trinitrophenyl-substituted nucleotides are potent antagonists selective for P2X$_1$, P2X$_3$, and heteromeric P2X$_{2/3}$ receptors. *Mol. Pharmacol.* **1998**, *53*, 969–973.

(15) (a) Evans, R. J.; Lewis, C.; Buell, G.; Valera, S.; North, R. A.; Surprenant, A. Pharmacological characterization of heterologously expressed ATP-gated cation channels (P$_{2X}$ purinoceptors). *Mol. Pharmacol.* **1995**, *48*, 178–183. (b) Pintor, J.; King, B. F.; Miras-Portugal, M. T.; Burnstock, G. Selectivity and activity of adenine dinucleotides at recombinant P2X$_2$ and P2Y$_1$ purinoceptors. *Br. J. Pharmacol.* **1996**, *119*, 1006–1012. (c) Wildman, S. S.; King, B. F.; Burnstock, G. Zn^{2+} modulation of ATP-responses at recombinant P2X$_2$ receptors and its dependence on extracellular pH. *Br. J. Pharmacol.* **1998**, *123*, 1214–1220.

(16) Jacobson, K. A.; Kim, Y.-C.; King, B. F. In search of selective P2 receptor ligands: interaction of dihydropyridine derivatives at recombinant rat P2X$_2$ receptors. *J. Auto. Nerv. Syst.* **2000**, *81*, 152–157.

(17) Bo, X.; Fischer, B.; Maillard, M.; Jacobson, K. A.; Burnstock, G. Comparative studies on the affinities of ATP derivatives for P2X-purinoceptors in rat urinary bladder. *Br. J. Pharmacol.* **1994**, *112*, 1151–1159.

(18) Bültmann, R.; Starke, K. P2-purinoceptor antagonists discriminate three contraction mediating receptors for ATP in rat vas deferens. *Naunyn-Schmiedeberg's Arch. Pharmacol.* **1994**, *349*, 74–80.

(19) Brake, A. J.; Wagenbach, M. J.; Julius, D. New structural motif for ligand-gated ion channels defined by an ionotropic ATP receptor. *Nature* **1994**, *371*, 519–523.

(20) Simon, J.; Webb, T. E.; King, B. F.; Burnstock, G.; Barnard, E. A. Characterisation of a recombinant P2Y purinoceptor. *Eur. J. Pharmacol.* **1995**, *291*, 281–289.

(21) Chang, K.; Hanoka, K.; Kumada, M.; Takuwa, Y. Molecular cloning and functional analysis of a novel P2 nucleotide receptor. *J. Biol. Chem.* **1995**, *270*, 26152–26158.

(22) Communi, D.; Parmentier, M.; Boeynaems, J.-M. Cloning, functional expression and tissue distribution of the human P2Y$_6$ receptor. *Biochem. Biophys. Res. Commun.* **1996**, *222*, 303–308.

(23) Communi, D.; Robaye, B.; Boeynaems, J.-M. Pharmacological characterization of the human P2Y$_{11}$ receptor. *Br. J. Pharmacol.* **1999**, *128*, 1199–1206.

(24) Michel, A. D.; Grahames, C. B. A.; Humphrey, P. P. A. Functional characterization of P2 purinoceptors in PC12 cells by measurement of radiolabelled calcium influx. *Naunyn-Schmiedeberg's Arch. Pharmacol.* **1996**, *354*, 562–571.

(25) Seguela, P.; Haghigi, A.; Soghommonian, J.-J.; Cooper, E. A novel neuronal P2X ATP receptor ion channel with widespread distribution in the brain. *J. Neurosci.* **1996**, *15*, 448–455.

(26) Webb, T. E.; Feolde, E.; Vigne, P.; Neary, J. T.; Runberg, A.; Frelin, C.; Barnard, E. A. The P2Y purinoceptor in rat brain microvascular endothelial cells couple to inhibition of adenylate cyclase. *Br. J. Pharmacol.* **1996**, *119*, 1385–1392.

(27) Glänzel, M.; Bültmann, R.; Starke, K.; Frahm, A. W. Structure-activity relationships of novel P2-receptor antagonists structurally related to Reactive Blue 2. *Eur. J. Med. Chem.* **2005**, *40*, 1262–1276.

(28) Glänzel, M.; Bültmann, R.; Starke, K.; Frahm, A. W. Constitutional isomers of Reactive Blue 2 - selective P2Y-receptor antagonists? *Eur. J. Med. Chem.* **2003**, *38*, 30–12.
(29) Weyler, S.; Baqi, Y.; Hillmann, P.; Kaulich, M.; Hunder, A. M.; Müller, I. A.; Müller, C. E. Combinatorial synthesis of anilinoanthraquinone derivatives and evaluation as non nucleotide-derived $P2Y_2$ receptor antagonists. *Bioorg. Med. Chem. Lett.* **2008**, *18*, 223–227.
(30) Baqi, Y.; Atzler, K.; Köse, M.; Glänzel, M.; Müller, C. E. High-affinity, non nucleotide-derived competitive antagonists of platelet $P2Y_{12}$ receptors. *J. Med. Chem.* **2009**, *52*, 3784–3793.
(31) Hoffmann, K.; Baqi, Y.; Morena, M. S.; Glänzel, M.; Müller, C. E.; von Kügelgen, I. Interaction of new, very potent non-nucleotide antagonists with Arg256 of the human platelet $P2Y_{12}$-receptor. *J. Pharmacol. Exp. Ther.* **2009**, *331*, 648–655.
(32) Baqi, Y.; Lee, S.-Y.; Iqbal, J.; Ripphausen, P.; Lehr, A.; Scheiff, A. B.; Zimmermann, H.; Bajorath, J.; Müller, C. E. Development of potent and selective inhibitors of ecto-5′-nucleotidase based on an anthraquinone scaffold. *J. Med. Chem.* **2010**, *53*, 2076–2086.
(33) Baqi, Y.; Weyler, S.; Iqbal, J.; Zimmermann, H.; Müller, C. E. Structure-activity relationships of anthraquinone derivatives derived from bromaminic acid as inhibitors of ectonucleoside triphosphate diphosphohydrolases (E-NTPDases). *Purinergic Signalling* **2009**, *5*, 91–106.
(34) Iqbal, J.; Lévesque, S. A.; Sévigny, J.; Müller, C. E. A highly sensitive CE-UV method with dynamic coating of silica-fused capillaries for the monitoring of nucleotide pyrophosphatase/phosphodiesterase reactions. *Electrophoresis* **2008**, *29*, 3685–3693.
(35) Tuluc, F.; Bültmann, R.; Glänzel, M.; Frahm, A. W.; Starke, K. P2-receptor antagonists: IV. Blockade of P2-receptor subtypes and ecto-nucleotidases by compounds related to reactive blue 2. *Naunyn-Schmiedeberg's Arch. Pharmacol.* **1998**, *357*, 111–120.
(36) (a) Baqi, Y.; Müller, C. E. Synthesis of alkyl- and aryl-amino-substituted anthraquinone derivatives by microwave-assisted copper(0)-catalyzed Ullmann coupling reactions. *Nat. Protoc.* **2010**, *5*, 945–953. (b) Baqi, Y.; Müller, C. E. Catalyst-free microwave-assisted amination of 2-chloro-5-nitrobenzoic acid. *J. Org. Chem.* **2007**, *72*, 5908–5911.
(37) Glänzel, M.; Bültmann, R.; Starke, K.; Frahm, A. W. Members of the acid blue 129 family as potent and selective P2Y-receptor antagonists. *Drug Dev. Res.* **2003**, *59*, 64–71.
(38) Daly, J. W. Caffeine analogs: biomedical impact. *Cell. Mol. Life Sci.* **2007**, *64*, 2153–2169.
(39) Baqi, Y.; Müller, C. E. Rapid and efficient microwave-assisted copper(0)-catalyzed Ullmann coupling reaction: general access to anilinoanthraquinone derivatives. *Org. Lett.* **2007**, *9*, 1271–1274.
(40) Kalontarov, I. Ya.; Kiseleva, N. N.; Zhuravleva, I. V. Study of the thermal and oxidative thermal degradation of poly(vinyl alcohol) dyed with reactive dyes. *IATOAN* (*Izvestiya Akademii Nauk Tadzhikskoi SSR, Otdelinie Fiziko-Matematicheskikh i Geologo-Khimicheskikh Nauk*) **1978**, *1*, 97–102.
(41) Greaves, A. J.; Churchley, J. H.; Hutchings, M. G.; Phillips, D. A. S.; Taylor, J. A. A chemometric approach to understanding the bioelimination of anionic, water-soluble dyes by a biomass using empirical and semi-empirical molecular descriptors. *Wat. Res.* **2001**, *35*, 1225–1239.
(42) Rettinger, J.; Braun, K.; Hochmann, H.; Kassack, M. U.; Ullmann, H.; Nickel, P.; Schmalzing, G.; Lambrecht, G. Profiling at recombinant homomeric and heteromeric rat P2X receptors identifies the suramin analogue NF449 as a highly potent $P2X_1$ receptor antagonist. *Neuropharmacology* **2005**, *48*, 461–468.
(43) Charlton, S. J.; Brown, C. A.; Weisman, G. A.; Turner, J. T.; Erb, L.; Boarder, M. R. Cloned and transfected $P2Y_4$ receptors: characterization of a suramin and PPADS-insensitive response to UTP. *Br. J. Pharmacol.* **1996**, *119*, 1301–1303.
(44) Hillmann, P.; Ko, G.-Y.; Spinrath, A.; Raulf, A.; von Kügelgen, I.; Wolff, S. C.; Nicholas, R. A.; Kostenis, E.; Höltje, H.-D.; Müller, C. E. Key determinants of nucleotide-activated G protein-coupled $P2Y_2$ receptor function revealed by chemical and pharmacological experiments, mutagenesis and homology modeling. *J. Med. Chem.* **2009**, *52*, 2762–2775.
(45) Kaulich, M.; Streicher, F.; Mayer, R.; Müller, I.; Müller, C. E. Flavonoids - novel lead compounds for the development of $P2Y_2$ receptor antagonists. *Drug Dev. Res.* **2003**, *59*, 72–81.
(46) Duckwitz, W.; Hausmann, R.; Aschrafi, A.; Schmalzing, G. P2X5 subunit assembly requires scaffolding by the second transmembrane domain and a conserved aspartate. *J. Biol. Chem.* **2006**, *51*, 39561–39572.
(47) Leisgen, C.; Kuester, M.; Methfessel, C. The roboocyte: automated electrophysiology based on Xenopus oocytes. *Methods Mol. Biol.* **2007**, *403*, 87–109.